# A Non-Intrusive Low-Cost Kit for Electric Power Measuring and Energy Disaggregation

Randy Quindai, Bruno M. Barbosa, Charles M. P. Almeida, Heitor S. Ramos, Joel J. P. C. Rodrigues, and Andre L. L. Aquino

***Abstract*—This article presents a kit to collect data of electric loads of single and three phases main power supply of a house and perform the energy disaggregation. To collect the data, we use sensors based on an open magnetic core to measure the electromagnetic field induced by the current in the electric conducting wire in a non-intrusive way. In particular, each sensor from the three-phase device wraps/encloses each phase without alignment. To calibrate the three-phase device, we present a method to calculate the neutral RMS without complex numbers using (Analysis of Variance) ANOVA and post hoc Tukey's multiple comparison tests to assert the differences of measures among phases. We managed to validate the method using a measure reference. Additionally, to perform the energy disaggregation, we use the NILMTK tool. This tool compares disaggregation algorithms on many public datasets. We use in our system two disaggregation algorithms Combinatorial Optimization and Factorial Hidden Markov Model algorithms. The results show that is possible to collect and perform energy disaggregation through our embedded system.**

***Index Terms*—Energy disaggregation, NilmTK, data acquisition, load monitoring.**

## I. Introduction

We observe a new area arousing interests in the scientific community, NILM disaggregation applications [1], [2], [3] that discusses techniques for event detection [4], [5], [6] that estimates the consumption of devices operating in different bands of energy consumption. These studies focus on residential, commercials and industries consumers. Several initiatives propose pointing this issue, such as the International Protocol for Measurement and Verification of Energy Performance (EVO - http://evo-world.org/en/), National Electric Energy Agency (ANEEL - http://www.aneel.gov.br/) and Energy research company (EPE - http://www.epe.gov.br/Paginas/default.aspx).

Nowadays, technologies for electric loads measurement have been focused on individual consumption, not addressing the consumers habits. These devices, best known as smart meters, can measure active, reactive and apparent power, as well as voltage and current. Besides, they provide a non-volatile memory to store the measures, for instance, Vector PAR Nansen [7], Kill A Watt [8], Power-Mate [9], among others.

Energy disaggregation is the process of estimating individual appliances consumption, given a full signal of power demand. There is not a standard for appliances consumption across the world. Different signatures patterns demand specific datasets for each country. NILMTK [10] uses these datasets through a personalized converter [11].

The literature presents many studies on energy disaggregation. Some of them focus on estimating the consumption of appliances operating in a different band of energy [4], [5], [6]. There are some tools to assist these studies, for instance, hidden Markov models [12], [5], fuzzy systems [6], [13] and evolutionary algorithms [14], [15]. Such studies are based on a set of data, listed here: *Building-Level fUlly-labeled dataset for Electricity Disaggregation* (BLUED) [16], *UK recording Domestic Appliance-Level Electricity* (UK-DALE) [17], *Reference Energy Disaggregation Data Set* (REDD) [12], *Smart** [17].

This article extends the study about the sensor kit proposed by Quindai et al. [18]. This kit makes available electric loads data by an open source electronic platform in such a way that monitors electrical loads and disaggregation studies. The disaggregation capability is the main contribution of the presented paper. Our kit can deliver data in real-time for NILM applications, that demands an enormous amount of data for disaggregation process, this data is stored in non-volatile memory and used for further analysis.

Besides that, it is presented an approach to calibrate non-intrusive sensors when measuring three-phase electric current. This calibration process allows a reduction of $\pm 1,4\%$ on errors on the data, occurred at discrepancy read due to offset circuitry connecting the Arduino to the sensors. There is, in literature, some calibration approaches considering the alignment of sensors in two wires conductors [19], [20] and at one wire conductors without alignment [21], [22], [23].

The organization of this article is as follows: Section II presents the single-phase and three-phase devices; Section III presents details about the variance analysis on the three-phase device; Section IV presents our Dataset Converter and the disaggregation results, and Section V conclusions and future works.

Manuscript received January 17, 2018; revised January 30, 2018. Date of publication March 15, 2018.

R. Quindai, B. Barbosa, C. Almeida, H. Ramos, and A.Aquino were with the Computer Institute of Federal University of Alagoas, Maceió, Alagoas, Brazil. E-mail: {randy.quindai, bruno.mb, charles.mariano, heitor, alla}@laccan.ufal.br

Joel J. P. C. Rodrigues was with National Institute of Telecommunications (Inatel), Santa Rita do Sapucaí - MG, Brazil,Instituto de Telecomunicações, Portugal, and University of Fortaleza (UNIFOR), Fortaleza - CE, Brazil. Email: joeljr@ieee.org

Digital Object Identifier (DOI): 10.24138/jcomss.v14i1.447

## II. The Non Intrusive Sensor Devices

Based on Arduino [24] technology, we develop a single-phase and three-phase devices, for the acquisition of electric current signal, they measure only effective current.

### A. *Single-phase meter*

For the **single-phase device**, it was used the current sensor SCT013 20 A/1 V (http://www.yhdc.com/, last access March 09th 2017). This SCT013 model accepts a maximum of 20A (twenty amps of alternate current), which suffices for typical home appliances. The current sensor provides a short range signal of the output voltage, which is proportional to the voltage at the input.

An Ethernet shield with a memory card slot (https://www.arduino.cc/en/Main/ArduinoEthernetShield) connected to Arduino is used to save the data into a memory card. The memory card has a capacity of 16GB, formatted with FAT file system. Data are stored in CSV format having the following columns: $I_{rms}$, $date$ and $miliseconds$; $I_{rms}$, which correspond to the value of effective current and date is in UTC-0300 format.

To conceive the single-phase collector device we used the Arduino UNO R3, connected to a SCT013 sensor and a real-time clock (RTC - Tiny DS1307), illustrated at Figure 1(a). Finally, Figure 1(b) shows the connection schema between the components: Arduino, current sensor, RTC, resistors, capacitor, and breadboard.

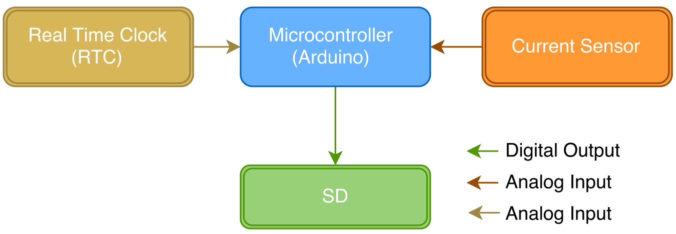


(a) Connections of the collector

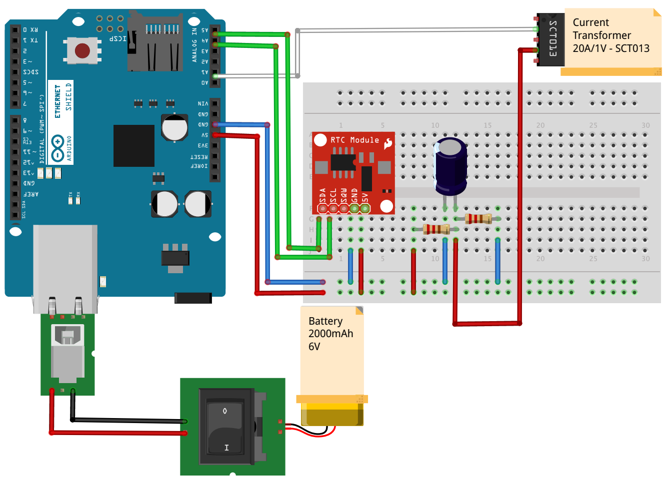


(b) Wiring Schema

Figure 1. Connections of the single-phase collector device and Wiring Schema.

TABLE I presents the number of equipment monitored. We collect all the data without interfering the regular use of appliances. For example, the data of coffee machine were gathered only in sufficient time to make the coffee and to keep the coffee hot. However, we collect the fridge data on a daily basis. The acquisition rate is about 10 Hz, which average of 10 (ten) measurements per second.

Table I
Measurements by Equipment.

| Measurements | | Measurements | |
|---|---|---|---|
| Appliances | Qty. | Appliances | Qty. |
| Apple TV | 1 | Washing machine | 2 |
| Air conditioner | 3 | Water machine | 2 |
| Coffee machine | 1 | Chuveiro | 2 |
| Air cleaner | 1 | DVD player | 1 |
| Squeezer | 1 | Iron | 1 |
| Electric Stove | 1 | Fridge | 2 |
| iMac27 | 1 | iPad Air 2 | 1 |
| iPhone 6 Plus | 1 | Fluorescent Lamp | 1 |
| Blender | 1 | Macbook Air 13 | 3 |
| Microwave | 1 | MiniSystem | 1 |
| Pool engine | 1 | Electric gate | 1 |
| Cable TV Receiver | 1 | Router | 1 |
| Eletr Grill | 1 | TV 32 LCD | 1 |
| TV 42 LED | 1 | Fan | 2 |

We save the data in different files for each equipment in the CSV format containing three columns: i) Effective electric current; ii) Time in UNIX timestamp format; iii) Milliseconds, for better precision. Table II shows one of our first measures. Observe that for each timestamp interval (1 second) the system measure the average of 10 different values.

Table II
Equipment Measurements Data Example.

| Fridge - CSV File | | |
|---|---|---|
| Effective Current (A) | Timestamp | milliseconds |
| 0.02 | 1442132519 | 996 |
| 9.31 | 1442132520 | 219 |
| 8.74 | 1442132520 | 441 |
| 8.45 | 1442132520 | 659 |
| 8.31 | 1442132520 | 878 |

Time series plots of the usage period for each equipment were generated *(effective current x time)* based on the collected data set. Through these plots, it is possible to analyze the equipment behavior concerning electric current in time. Figure 2 shows some examples of electric current plots for air-conditioner (Figure 2(a)), washing machine 2(b), and electric shower 2(c).

This collector has potential to produce data sets for load characterization and energy disaggregation applications. Usually, these data sets available at literature reports two types of measures: i) main power supply of the house collected in high-frequency (values above 1 kHz), and ii) device socket level collected in low-frequency. Our device is compatible with this standard.

### B. *Three-phase meter*

The Energy Meter described here was developed using an Arduino, a real-time clock (RTC) and three current trans-

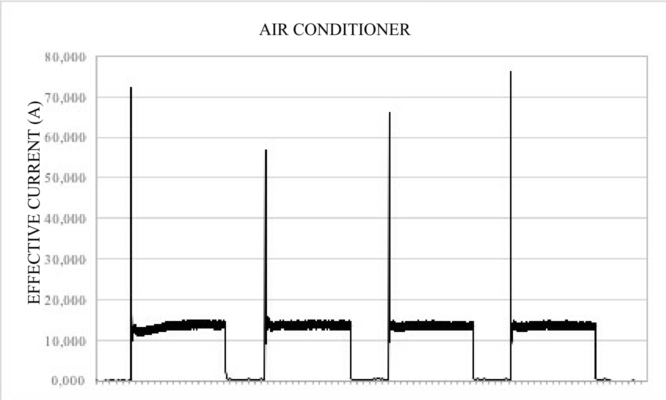


(a) Air conditioner

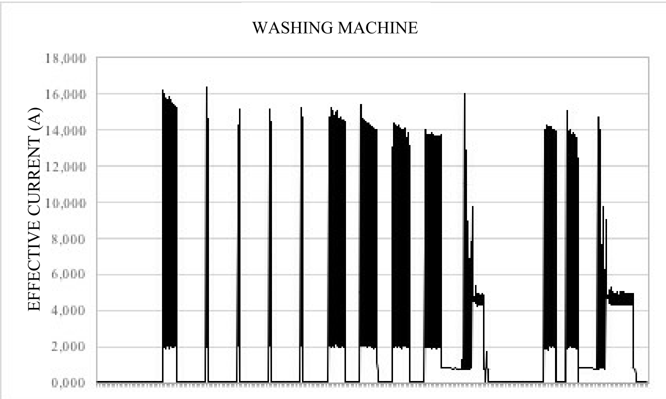


(b) Washing Machine

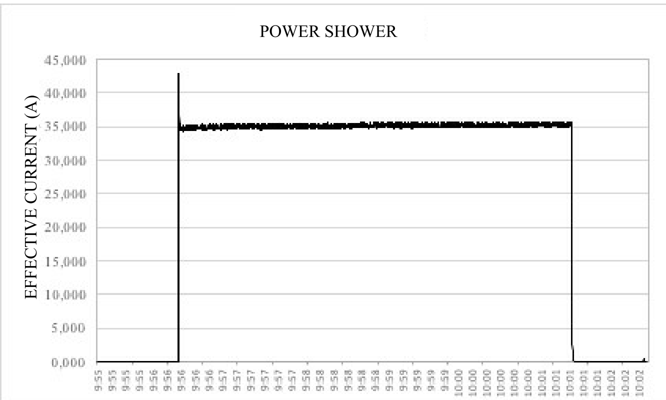


(c) Power Shower

Figure 2. Consumption curves for different appliances.

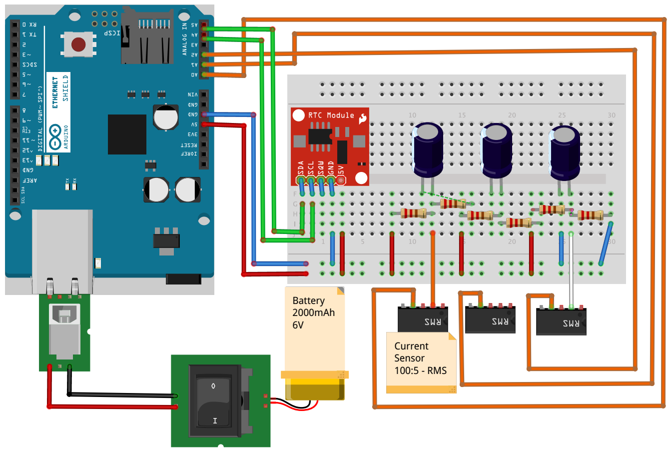


(a) Wiring Schema

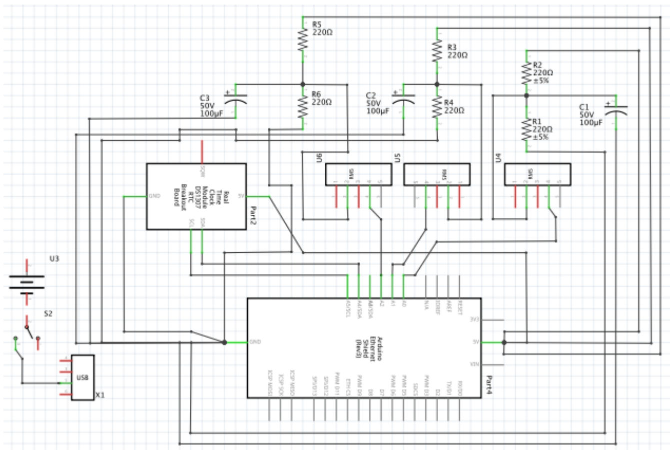

(b) Electronic Schema

Figure 3. Energy Meter Device Connections and Wiring Schema.

formers. In this way, to perform measurements in multiphasic systems, it is necessary to use several current transformers (CT), one for each phase, where just a single error in one of them could lead to significant measurement errors.

Figure 3(a) presents the device wiring schema. We have an Arduino UNO R3, a Shield Ethernet connected to Arduino, as shown in Figure 3(b), three offset circuits of passive elements, one for each CT, a battery, a clock counter and three CTs PA_ALI3MN10100A [25] with maximum diameter of 20 mm and power scale from 10 A to 100 A.

The RMS mentioned above CT, comes with a male connector XLR that was adapted to connect to Arduino's analog gates A0, A1, and A2 respectively for each CT, where one extremity connects one resistive circuit and the other one on the Arduino. This CT provides a voltage signal in secondary of CT to Arduino, alternating between positive and negative values, however, Arduino only accepts positive values with the maximum voltage of 5 V. To overcome this issue, we use an offset circuit, which only allows the current signal to positive values 2 V peak-to-peak. A resistive divider and a capacitor compose this circuit, amplifies the parasite capacitance effects in high rate acquisitions, producing a small discrepancy at CT's signal in the output, therefore, to reduce the noise an adjustment was necessary. This device measures effective electric current with a rate of 3 Hz. We use the library EmonTx[26] from OpenEnergyMonitor to communicate the Arduino to sensors.

We store the data measured in a sd card formatted with FAT file system, similar to the single-phase device. The data set has the following columns: $I_{rms,0}$, $I_{rms,1}$, $I_{rms,2}$, $date$ and $milliseconds$, where the time is in UTC-0300 format and, $I_{rms,j}$ is the effective current at $TC_j$, where $j = 0 \ldots 2$. This device power is through USB type B with four batteries, this port has a current limitation of 250$\sim$500 mA h.

For the system autonomy, we consider four ways to power on the Arduino: i) Jack plug with input voltage of 7∼12 V; ii) Vin pin with input voltage of 6∼12 V; iii) 5 V pin; iv) USB Type B port of 5 V; It is discarded the Vin pin because it is not protected for polarity change and could create conflicts with Jack plug, damaging the Arduino board. The 5 V pin is connected directly to the output regulator, with a stable power supply. Hence, the Arduino can be powered safely, since there is no current at Jack or USB port. It is recommended to use Jack plug with a current of 250∼500 mA h or USB type B port.

## III. Analysis of Data Variance and Calibration

The signal received by the Arduino was conditioned, needed to be corrected, for such it is calculated a parameter such that the output signal becomes balanced to the input signal. In practice, systems rarely have perfectly balanced loads, currents, voltages, and impedances in all three phases. We determine the neutral current by adding the three-phase currents together as complex numbers and then converting from rectangular to polar coordinates. It will be presented a method to calculate the neutral RMS without complex numbers.

The method consists of finding a constant number using a known power. To calculate this parameter, we use a circuit of 5 lamps of 40 W connected in parallel, and then we measure the current of the circuit with the Agilent U3401 [27] multimeter, which is a high standard multimeter. We put the tips of the multimeter in series to lamps circuit in about two minutes. Table III, shows the current measured with the multimeter (Real), the same current measured with our device (Meter), and the proportion between them (Real/Meter). The constant $w$ is the mean of the column Real/Meter. To calibrate by software one just need to multiply $w$ to the output signal for each sensor connected to Arduino.

Table III
Calculus of Constant ($w$) for each CT Output Signal.

| Nº Lamps | Current(A) Real | Mean Meter (with offset) | Real/Measured |
|---|---|---|---|
| 1 | 0.1764 | 2.33675159235669 | 0.0754894104178591 |
| 2 | 0.360 | 4.72190476190476 | 0.076 |
| 3 | 0.546 | 7.08077669902912 | 0.0771101848297045 |
| 4 | 0.726 | 9.33976076555023 | 0.0777321837490587 |
| 5 | 0.902 | 11.6576834862385 | 0.077373862574394 |

The boxplot in Figure 4, is the current collector with our device without calibration. The current is different in each sensor, even measuring the same current at the same time. We hypothesize that the average is different for each sensor. Thus we use the ANOVA test with significance level of $\alpha = 0.05$ to confirm it:

$H_0$: the data load average is the same for the three sensors, that is, $\mu_{s0} = \mu_{s1} = \mu_{s2}$, considering that any differences are due to chance.

$H_A$: at least one mean is different.

Our sample has $df_G = k - 1$ degrees of freedom, where $k$ is the number of sensors, $H_0$ null hypothesis, $\mu_{s_j}$ the mean on sensor $j$ and, $H_A$ the alternative hypothesis. We use R to perform all computations. Statistics of the three-phases are present in Tables IV and V, where one can observe the variance, standard deviation, and standard error.

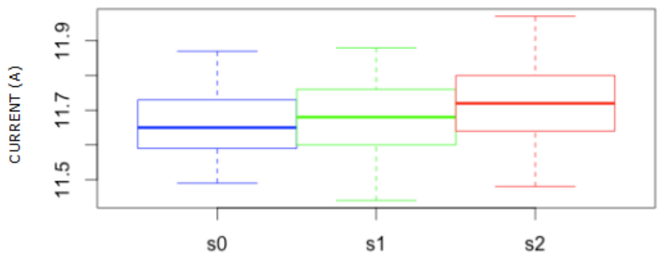

Figure 4. Current collected data without calibration.

Table IV
Statistical Parameters (5 lamps circuit).

| | Sensor $S_0$ | $S_1$ | $S_2$ |
|---|---|---|---|
| $n$ | 100 | 100 | 100 |
| Average | 11.6629 | 11.6727 | 11.7125 |
| $\sigma^2$ | 0.0076 | 0.0091 | 0.0104 |
| SD | 0.0869 | 0.0951 | 0.1020 |
| SE | 0.0087 | 0.0095 | 0.0102 |

Table V
Resume of ANOVA (without calibration).

| | df | Sum of squares (SQ) | Mean Square (MS) | F | P (>F) |
|---|---|---|---|---|---|
| Between sensors | 2 | 0.138 | 0.069 | 7.666 | 0.000567 |
| Within sensor /Residuals | 297 | 2.674 | 0.009 | | |

Observe that in Table IV, $n$ is the sample size, $\sigma^2$ the variance, SD the standard deviation and SE the standard error, individually for each CT($S_j$). Table V shows the ANOVA results for each CT, noting the p-value <0.05.

We reject the null hypothesis. The ANOVA test shows that there is at least one average different. To verify this, we conduct a post hoc analysis, after prior analysis of the data, an inspection was performed to find the patterns. Using Tukey's HSD test with confidence level equal to 0.95, we computed the differences in averages. Since the sample has the same size, the Type 1 error is precisely the significance level $\alpha = 0.05$.

Table VI and Figure 5(a) shows the differences using the TukeyHSD method (Tukey Honest Significant Differences), we do not reject the null hypothesis because the p-value lies between $s_1$-$s_0$, but, we cannot assure that the same happens on others two comparisons. Table VII, the TukeyHSD test was repeated after calibration of the sensors. Observe that we fail to reject the null hypothesis in all cases. Our device needs calibration, as can be observed at Table VII and Figure 5(b). However, after the software-based calibration performed by the Arduino board, using the constant $w$ calculated above, the center of the confidence intervals becomes closer diminishing the overlapping gap.

Table VI
TUKEYHSD APPLIED TO SAMPLE BEFORE CALIBRATION.

| sensor | diff | $lim_inferior$ | $lim_superior$ | P |
|---|---|---|---|---|
| $s_1$-$s_0$ | 0.0098 | -0.021805667 | 0.04140567 | 0.7456582 |
| $s_2$-$s_0$ | 0.0496 | 0.017994333 | 0.08120567 | 0.0007587 |
| $s_2$-$s_1$ | 0.0398 | 0.008194333 | 0.07140567 | 0.0091169 |

Table VII
TUKEYHSD AFTER CALIBRATION.

| sensor | diff | $lim_inferior$ | $lim_superior$ | P |
|---|---|---|---|---|
| $s_1$-$s_0$ | 0.005060310 | -0.04289750 | 0.05301812 | 0.9665233 |
| $s_2$-$s_0$ | 0.014354013 | -0.03360379 | 0.06231182 | 0.7607118 |
| $s_2$-$s_1$ | 0.009293703 | -0.03866411 | 0.05725151 | 0.8915578 |

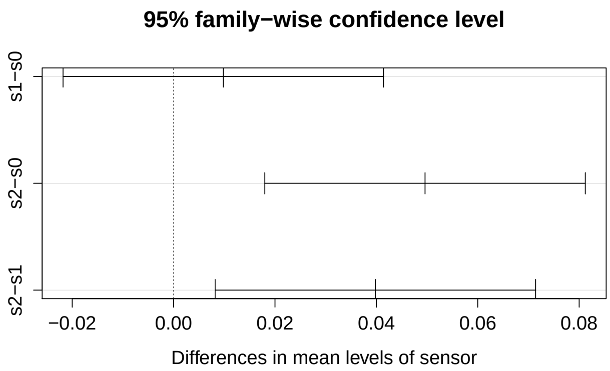


(a) Data before calibration

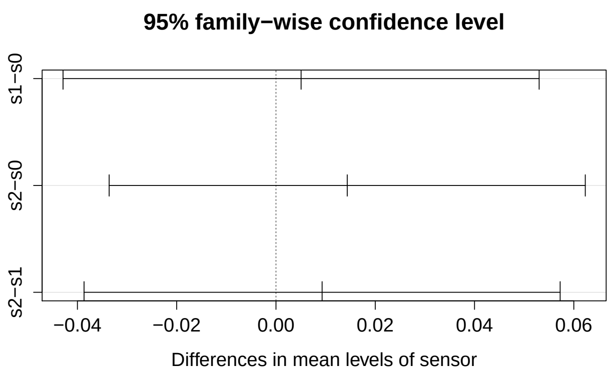


(b) Data after calibration

Figure 5. Confidence intervals before and after calibration.

Using R, we collected a random sample of size 100 of the prior data collected, for each sensor, $s_0$, $s_1$ and $s_2$ respectively.We fixed $s_0$ as a reference and compute the differences between $s_0$ and the others two sensors, we observed that the error can be described by the following distributions: E1$\sim$N($\mu$=0.0098, $\sigma$ = 0.1651567) and E2$\sim$N($\mu$=0.0496, $\sigma$ = 0.09982733), that describes the corrections $s_1$ and $s_2$ at sensors output signals. After calibration, as shown in Table VIII, we obtained the p-value more significant than the significance level ($\alpha = 0.05$), with this result we validate the distributions E1 and E2 and fail to reject the null hypothesis.

Table VIII
RESUME OF ANOVA AFTER CALIBRATION.

| | df | Sum of Squares (SQ) | Mean Square (MS) | F | P (>F) |
|---|---|---|---|---|---|
| Between sensors | 2 | 0.011 | 0.00530 | 0.256 | 0.775 |
| Within /Residuals | 297 | 6.156 | 0.02073 | | |

## IV. DATASET IMPORTER AND DISAGGREGATION TOOL

To provide energy disaggregation, we used NILMTK, which is a Python-based toolkit with the purpose of comparing disaggregation algorithms on many public datasets. Our focus was on disaggregation with Combinatorial Optimization (CO) and Factorial Hidden Markov Model (FHMM) algorithms. We use a data set collected through our devices from one house on a single day. In this case, we collected individual signatures through single-phase device and used previously for CO and FHMM training and calibration. After that, we use the three-phase device to obtain the main data and then to apply the disaggregation through CO and FHMM algorithms.

NILMTK provides many source code of dataset converters, and a metadata descriptor for energy disaggregation [11], these source codes convert data from public datasets to HDF5 format, which is the format recognized by the NILMTK. We based our converter on REDD converter. We called our dataset LAC, which is an abbreviation of LaCCAN, the lab which is our workplace. REDD converts to HDF5 DAT files, and the timestamp column contains 10-digit timestamps. Our dataset converter uses CSV files, and the timestamp column contains 13-digit timestamps when the three last digits are the milliseconds. Both convert input files to a *pandas* data frame and, through *pandas*, it is possible to decide how timestamp format to use. Besides, the HDF5 file includes metadata files, also presented in YAML files. They are descriptions of appliances in the house (in the `building1.yaml` file). This file defines which channel the appliance is in that house. The channel 1 is the main of the house, and the others are the appliances. The other files make descriptions of the dataset (in the `dataset.yaml` file) and descriptions of the equipment used to collect data (in the `meter_devices.yaml` file).

After converting CSV files to HDF5, the next step was the application of disaggregation algorithms on the data collected. We applied the FHMM and CO algorithms [28]. The experiment results are depicted on Figures 6 and 7 that shows the graphic of the consumption in the referred day. Figure 7 shows disaggregation using CO algorithm and figure 6 shows disaggregation using FHMM algorithm. Both CO and FHMM algorithm uses values obtained on channel 1 (red line), which is the main of the house, the other lines are individual

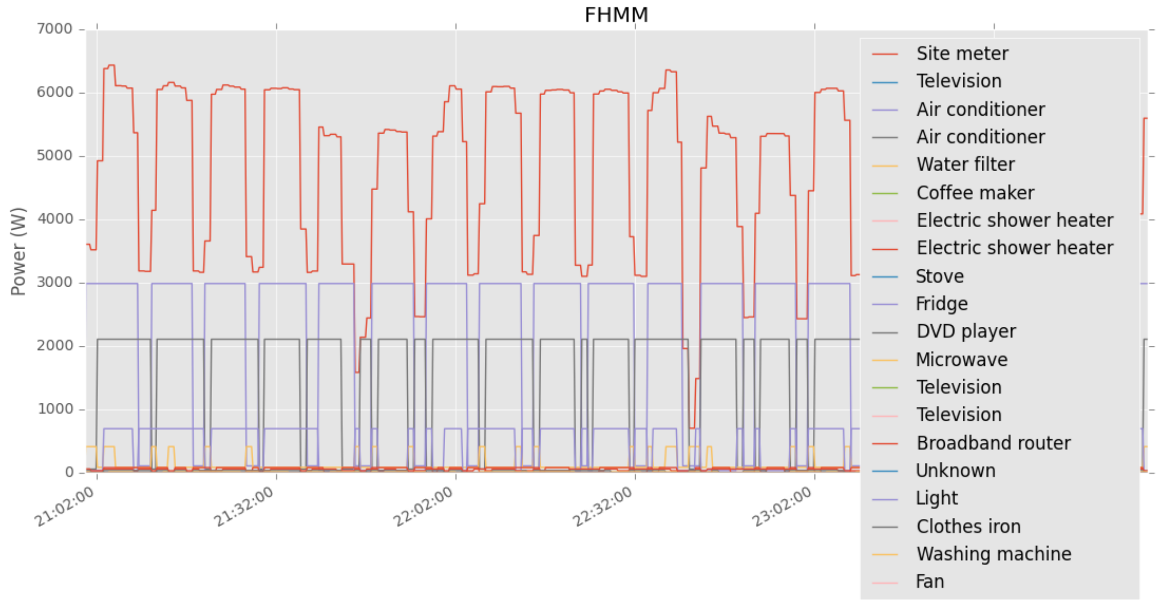


Figure 6. Disaggregation plot by FHMM algorithm.

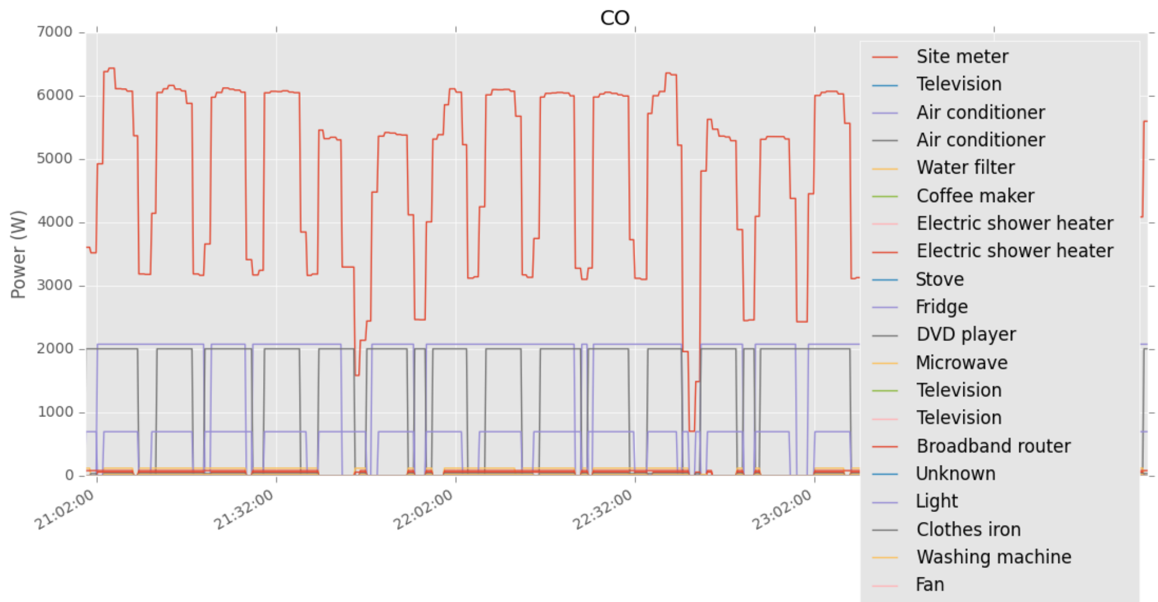


Figure 7. Disaggregation plot by CO algorithm.

consumption of each house appliance. So, they show us which appliance is using the main power by the main values. Note that on these examples the air conditioners are the devices that consume more. However, it is possible to identify differences between FHMM and CO.

Additionally, the Figures 8 and 9 show the accuracy of each disaggregation algorithm used, which shows how perfect was the prediction made by the algorithms. With this evaluation, we can identify that FHMM algorithm is better than CO. With FHMM we can obtain better results in air conditioners and water filter devices.

## V. Conclusion and Future Work

With the purpose of providing data to surveys disaggregation studies, load monitoring and better energy efficiency, we presented a three-phase device to collect electric loads data, section II-B, with a methodology to recover the real value of current measured after an offset performed required by the Arduino board.

Initially, the three-phase device presented a significant variance. Thus the calibration was performed through the method that calculates a constant value, avoiding the use of complex numbers to obtain the neutral RMS current. We validated the

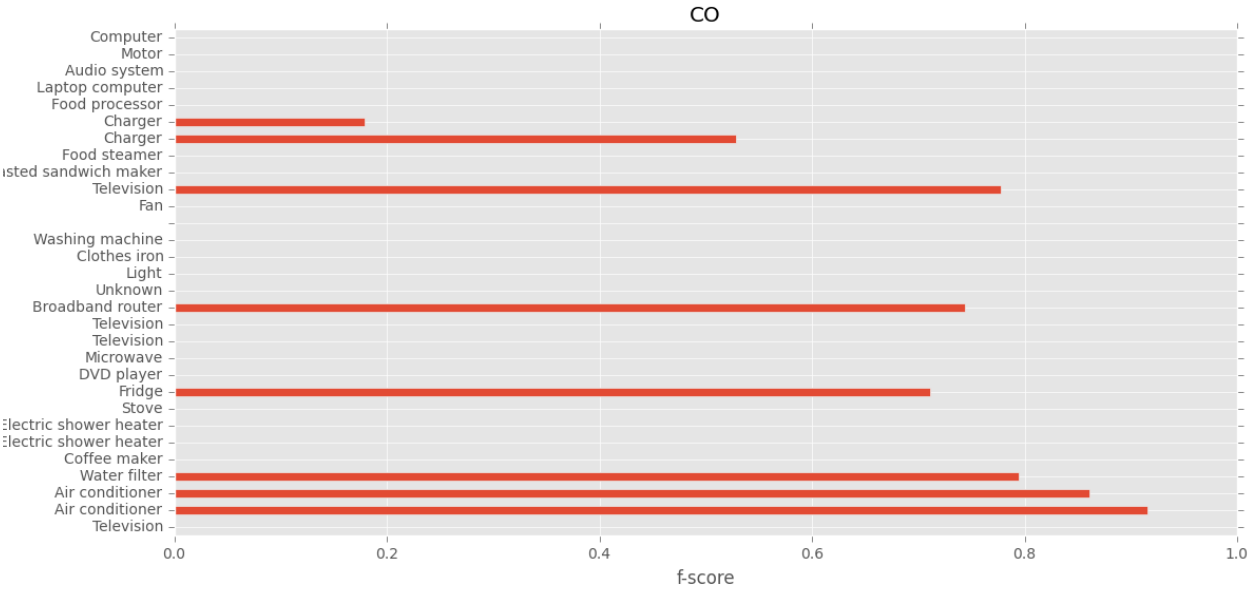


Figure 8. Accuracy of CO algorithm.

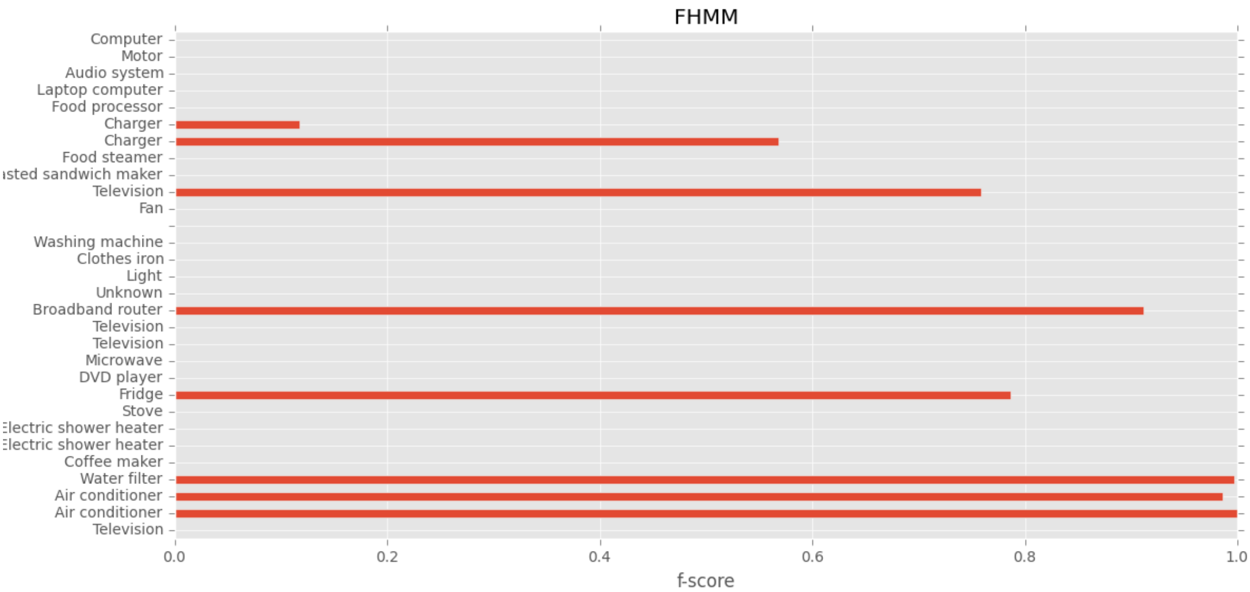


Figure 9. Accuracy of FHMM algorithm.

approach using ANOVA and TukeyHSD tests. This method is not limited to our device, and it can be used to calibrate any polyphasic device meter. We estimate that the distribution of errors follows a Gaussian distribution.

The single-phase and three-phase devices were constructed mainly to perform surveys on disaggregation studies using NILM, but, they can be used to implement smart measurement too. Finally, we show an accuracy comparison of FHMM and CO algorithms on our dataset, covering the gap on data acquisition for disaggregation studies with a low-cost Arduino-based kit.

As future work, the authors intent to develop studies on real-time disaggregation within a smart meter, investigate different disaggregation solution, now based on information theory concepts, and to use all solution embedded in a general proposing microcontroller.

## ACKNOWLEDGMENTS

We acknowledge support from CNPq, FAPEAL, and FAPESP, all Brazilian research agencies. This work was partially supported by National Funding from the FCT - Fundação para a Ciência e a Tecnologia through the UID/EEA/500008/2013 Project; by Brazilian National Council for Research and Development (CNPq) via Grant No.

309335/2017-5; by Finep, with resources from Funttel, Grant no. 01.14.0231.00, under the Radiocommunication Reference Center (Centro de Referência em Radiocomunicações - CRR) project of the National Institute of Telecommunications (Instituto Nacional de Telecomunicações - Inatel), Brazil.

## References


[1] S. B. Leeb, S. R. Shaw, and J. Kirtley, J. L., "Transient event detection in spectral envelope estimates for nonintrusive load monitoring," *IEEE Trans. Power Del.*, vol. 10, no. 3, pp. 1200–1210, 1995.

[2] K. S. Barsim, R. Streubel, and B. Yang, "An approach for unsupervised non-intrusive load monitoring of residential appliances," in *2nd Non-Intrusive Load Monitoring Workshop (NILM)*, 2014.

[3] K. Anderson, M. Berges, A. Ocneanu, D. Benitez, and J. Moura, "Event detection for non intrusive load monitoring," in *38th Annual Conference on IEEE Industrial Electronics Society (IECON)*, 2012, pp. 3312–3317.

[4] K. Anderson, J. M. F. Moura, and M. Berges, "Unsupervised approximate power trace decomposition algorithm," in *2nd Non-Intrusive Load Monitoring Workshop (NILM)*, 2014.

[5] O. Parson, S. Ghosh, M. Weal, and A. Rogers, "An unsupervised training method for non-intrusive appliance load monitoring," *Artificial Intelligence*, vol. 217, no. 1, pp. 1–19, 2014.

[6] Y.-H. Lin, M.-S. Tsai, and C.-S. Chen, "Applications of fuzzy classification with fuzzy c-means clustering and optimization strategies for load identification in NILM systems," in *IEEE International Conference on Fuzzy Systems (FUZZ-IEEE)*, 2011, pp. 859–866.

[7] Salfatis LTDA. (2016, Apr.) Salfatis website. http://salfatis.com.br, accessed on april 2016.

[8] P3 International. (2016, Apr.) P3 website. http://www.p3international.com, accessed on april 2016.

[9] CCI LTD. (2016, Apr.) Computer control instrumentation website. http://www.c-c-i.com.au/, accessed on april 2016.

[10] N. Batra, J. Kelly, O. Parson, H. Dutta, W. Knottenbelt, A. Rogers, A. Singh1, and M. Srivastava, "Nilmtk: An open source toolkit for non-intrusive load monitoring," in *5th International Conference on Future Energy Systems (ACM e-Energy)*, 2014.

[11] J. Kelly and W. Knottenbelt, "Metadata for energy disaggregation," in *2014 IEEE 38th International Computer Software and Applications Conference Workshops*, July 2014, pp. 578–583.

[12] J. Z. Kolter and M. J. Johnson, "REDD: A public data set for energy disaggregation research," in *1st KDD Workshop on Data Mining Applications in Sustainability (SustKDD)*, 2011.

[13] Y.-H. Lin and M.-S. Tsai, "Non-intrusive load monitoring by novel neuro-fuzzy classification considering uncertainties," *IEEE Trans. Smart Grid*, vol. 5, no. 5, pp. 2376–2384, 2014.

[14] D. Egarter, A. Sobe, and W. Elmenreich, "Evolving non-intrusive load monitoring," in *16th European Conference on Applications of Evolutionary Computation*, 2013, pp. 182–191.

[15] H.-H. Chang, L.-S. Lin, N. Chen, and W.-J. Lee, "Particle-swarm-optimization-based nonintrusive demand monitoring and load identification in smart meters," *IEEE Trans. Ind. Appl.*, vol. 49, no. 5, pp. 2229–2236, 2013.

[16] K. Anderson, A. Ocneanu, D. Benitez, D. Carlson, A. Rowe, and M. Berges, "BLUED: a fully labeled public dataset for Event-Based Non-Intrusive load monitoring research," in *2nd KDD Workshop on Data Mining Applications in Sustainability (SustKDD)*, 2012.

[17] J. Kelly and W. J. Knottenbelt, "The UK-DALE dataset, domestic appliance-level electricity demand and whole-house demand from five UK homes," *Scientific Data*, vol. 2, no. 1, p. 150007, 2015.

[18] R. Quindai, C. M. P. Almeida, H. S. Ramos, J. J. P. C. Rodrigues, and A. L. L. Aquino, "A non intrusive low cost arduino-based three phase sensor kit for electric power measuring," in *2nd International Multidisciplinary Conference on Computer and Energy Science (SpliTech)*, 2017.

[19] Y. C. Chen, W. H. Hsu, S. H. Cheng, and Y. T. Cheng, "Anti-electromagnetic interference and calibration schemes of flexible current sensor tag for reliable current detection in household appliance," in *Solid-State Sensors, Actuators and Microsystems (TRANSDUCERS EUROSENSORS XXVII), 2013 Transducers Eurosensors XXVII: The 17th International Conference on*, June 2013, pp. 1356–1359.

[20] J. Zhang, Y. Wen, and P. Li, "Nonintrusive current sensor for the two-wire power cords," *IEEE Transactions on Magnetics*, vol. 51, no. 11, pp. 1–4, Nov 2015.

[21] N. Tamkittikhun, T. Tantidham, and P. Intakot, "Ac power meter design for home electrical appliances," in *Electrical Engineering/Electronics, Computer, Telecommunications and Information Technology (ECTI-CON), 2015 12th International Conference on*, June 2015, pp. 1–6.

[22] B. Campbell and P. Dutta, "Gemini: A non-invasive, energy-harvesting true power meter," in *Real-Time Systems Symposium (RTSS), 2014 IEEE*, Dec 2014, pp. 324–333.

[23] G. Crotti, D. Gallo, D. Giordano, C. Landi, and M. Luiso, "A characterized method for the real-time compensation of power system measurement transducers," in *Precision Electromagnetic Measurements (CPEM 2014), 2014 Conference on*, Aug 2014, pp. 730–731.

[24] Arduino LLC. (2016, Mar.) Arduino website. http://www.arduino.cc/, accessed on march 2016.

[25] RMS Sistemas Eletrônicos. (2016, Apr.) Rms website. http://rms.ind.br, accessed on april 2016.

[26] Open Energy Monitor. (2016, Mar.) Open energy monitor coorporation website. http://openenergymonitor.org, accessed on march 2016.

[27] Keysight. (2016, Apr.) Keysight. http://www.keysight.com, accessed on april 2016.

[28] N. Batra, *Comparing FHMM and CO*. [Online]. Available: https://github.com/nilmtk/nilmtk/blob/master/notebooks/co_fhmm.ipynb


**Randy A. Quindai** is an undergraduate student at the Federal University of Alagoas - Brazil, enrolled in Computer Science program and is a member of Laboratório de Computação Científica e Análise Numérica - LaCCAN, at Federal University of Alagoas - UFAL.

**Charles M. P. Almeida** is an Electrical Engineer graduated at Federal University of Pernambuco - UFPE, 2005. Specialist in labor safety engineering at the Centro Universitário de Volta Redonda - UNIFOA, 2007. Project specialist, execution & control of electrical engineering by the Institute of postgraduate and undergraduate studies - IPOG, 2017. Currently, is working as a forensics expert in Electrical Engineering at Official Expertise of the State of Alagoas - POAL. He is a member of Laboratório de Computação Científica e Análise Numérica - LaCCAN, at Federal University of Alagoas - UFAL.

**Bruno M. Barbosa** is an undergraduate student at the Federal University of Alagoas - Brazil, enrolled in Computer Engineering program and is a member of Laboratório de Computação Científica e Análise Numérica - LaCCAN, at Federal University of Alagoas - UFAL.

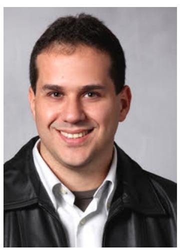

**Heitor S. Ramos** is graduated in Electrical Engineering from the Federal University of Campina Grande, Brazil. His master in Computing Modeling from the Federal University of Alagoas, Brazil, and his Ph.D. in Computer Science from the Federal University of Minas Gerais. His research interests rely on wireless networks, sensors networks, mobile and ad hoc networks, and urban computing. He is currently a Professor at the Institute of Computing of the Federal University of Alagoas, Maceió, Brazil.

**Joel J. P. C. Rodrigues** [S'01, M'06, SM'06] is a professor and senior researcher at the National Institute of Telecommunications (Inatel), Brazil and senior researcher at the Instituto de Telecomunicações, Portugal. Prof. Rodrigues is the leader of the Internet of Things research group (CNPq), Director for Conference Development - IEEE ComSoc Board of Governors, IEEE Distinguished Lecturer, the President of the scientific council at ParkUrbis – Covilhã Science and Technology Park, the Past-Chair of the IEEE ComSoc Technical Committee on eHealth, the Past-chair of the IEEE ComSoc Technical Committee on Communications Software, Steering Committee member of the IEEE Life Sciences Technical Community and Publications co-Chair, and Member Representative of the IEEE Communications Society on the IEEE Biometrics Council. He is the editor-in-chief of three International Journals and editorial board member of several high-reputed journals. He has been general chair and TPC Chair of many international conferences, including IEEE ICC, IEEE GLOBECOM, and IEEE HEALTHCOM. He has authored or coauthored over 550 papers in refereed international journals and conferences, 3 books, and 2 patents. He had been awarded several Outstanding Leadership and Outstanding Service Awards by IEEE Communications Society and several best papers awards. Prof. Rodrigues is a licensed professional engineer (as senior member), member of the Internet Society, and a senior member ACM and IEEE.

**Andre L. L. Aquino** is a Professor at Federal University of Alagoas, Brazil. He received his Ph.D. in Computer Science from the Federal University of Minas Gerais, Brazil, in 2008. His research interests include data reduction, distributed algorithms, wireless ad hoc and sensor networks, mobile and pervasive computing. Besides, he has published several papers in the area of wireless sensor networks.